Highly Dispersed Rhodium Particles on SiO_2 and β-FeOOH Supports Formed by Photochemical Decomposition of a Rh(I) Compound

Zhibang Duan and Mark J. Hampden-Smith*

Department of Chemistry and Center for Micro-Engineered Ceramics, University of New Mexico, Albuquerque, New Mexico 87131

Received March 10, 1993. Revised Manuscript Received May 4, 1993

The preparation of 2-4-nm-sized Rh particles dispersed on amorphous SiO_2 and crytalline β-FeOOH at room temperature by photochemical decomposition of $[(C_2H_4)_2Rh(OEt)]_2 \cdot H_2O$ is described. Tetrahydrofuran solutions of the Rh precursor containing either 250 nm sized SiO_2 spheres or 250 × 55 nm single-crystal β-FeOOH rod-shaped particles were irradiated for 3 h with a Hg arc lamp. Transmission electron microscopy, energy dispersive spectroscopy and electron diffraction revealed that 2-4-nm-sized crystalline Rh particles were dispersed on the surface of the metal oxide particles with a Rh weight loading which corresponded closely to the solution Rh content. A series of control experiments in which the rate of photochemical decomposition of $[(C_2H_4)_2Rh(OE)]_2 \cdot H_2O$ was monitored by ^1H NMR spectroscopy revealed that the precursor reacted in homogeneous solution rather than on the surface of the metal oxide. This represents a convenient method for the preparation of highly dispersed catalyst particles on thermally sensitive substrates.

Introduction

The preparation of highly dispersed metal particles can be achieved by a variety of chemical and physical techniques. Typical preparation methods include metal evaporation, metal-organic decomposition, and chemical or photochemical reduction of metal complexes.[1-12] When metal complexes are used as precursors, methods to control particle size generally require the use of surfactants, which may reduce the reactivity of the metal.[13] In heterogeneous catalysis applications, the active metal is normally dispersed on a metal oxide support such as SiO_2 or TiO_2. Preparation methods such as impregnation, coprecipitation and ion exchange, based on the use of metal complexes, generally require calcination and reduction processes.[14] During the calcination process, oxidation to remove the organic ligands can also oxidize the metal to form the metal oxide.[15] As a result, oxidation is usually followed by a reduction step to form the active metal. However, the relatively high temperature required for these steps[15,16] can cause aggregation of the metal catalyst particles, resulting in changes in size-dependent properties such as activity and selectivity[17] and can also lead to changes in the microstructure of the metal oxide support.[18] These microstructural changes can adversely affect the surface area and porosity, as well as chemical properties of the support material. Furthermore, high-temperature reduction processes make some supports such as FeOOH and Fe_2O_3 inaccessible. These supports can exhibit a strong influence in catalytic reactions. For example, gold, which has attracted little attention itself as a catalyst, when supported on α-Fe_2O_3, Co_3O_4, and NiO, exhibits high catalytic activity for the oxidation of CO, even at -70 °C.[19]

Photochemical decomposition of organometallic precursors seems a viable alternative to produce metal particles at low temperature. The photodeposition method has been used to form oxide-supported metal particles for some time.[20-22] Most studies have required additional reagents to promote reduction of the metal-containing precursor to colloidal metal. In aqueous systems, the chromophore is often the support surface. This has been used to advantage for selective deposition of a metal catalyst on a photoactive, semiconductor support with a suitable bandgap, in the presence of a photoinactive (insulating) support.[20,22] For example, photochemically

* To whom correspondence should be addressed.

(1) Davis, R. C.; Klabunde, K. J. *Chem. Rev.* **1982**, *82*, 153.
(2) Brauer, G. *Handbook of preparative Inorganic Chemistry*, 2nd ed.; Academic: New York, 1965; Vol. 2.
(3) Rieke, R. D. *Science*, **1989**, *246*, 1260.
(4) Bönnemann, H.; Brijoux, W.; Joussen, T. *Angew. Chem., Int. Ed. Engl.* **1990**, *29*, 273.
(5) Bönnemann, H.; Brijoux, W.; Brinkmann, R.; Dinjus, E.; Korall, B. *Angew. Chem., Int. Ed. Engl.* **1991**, *30*, 1312.
(6) Bradley, J. S.; Millar, J. M.; Hill, E. W.; Behal, S. *J. Catal.* **1991**, *129*, 530:
(7) Bradley, J. S.; Millar, J. M.; Hill, E. W.; Melchior, M. *J. Chem. Soc., Chem. Commun.* **1990**, 705.
(8) Bradley, J. S.; Millar, J. M.; Hill, E. W. *J. Am. Chem. Soc.* **1991**, *113*, 4016.
(9) Duan, Z.; Hampden-Smith, M. J.; Datye, A.; Nigrey, P.; Quintana, C.; Sylwester, A. P. *Mater. Res. Soc. Symp. Proc.* **1992**, *272*, 109.
(10) Duan, Z.; Hampden-Smith, M. J.; Datye, A.; Nigrey, P.; Quintana, C.; Sylwester, A. P. *J. Catal.* **1993**, *139*, 504.
(11) Duan, Z.; Hampden-Smith, M. J.; Sylwester, A. P. *J. Organomet. Chem.* **1993**, *449*, 173.
(12) Glassl, H.; Hayek, R.; Kramer, R. *J. Catal* **1981**, 68, 397.
(13) (a) Wilcoxon, J. P.; Williams, R. L. *Mater. Res. Soc. Proc.* **1990**, *169*, 17. (b) Ohtaki, M.; Toshima, N. *Chem. Lett.* **1990**, 489.
(14) Campbell, I. M. In *Catalysis at Surfaces*; Chapman Hall: New York, 1988.
(15) See, e.g.: Breitscheidel, B.; Zieder, J.; Schubert, U. Schubert, *Chem. Mater.* **1991**, *3*, 559 and references therein.
(16) Poston, S.; Reisman, A. *J. Electron. Mater.* **1989**, *18*, 553.
(17) Che, M.; Bennett, C. O. *Adv. Catal.* **1989**, *36*, 55.
(18) Brinker, C. J.; Scherer, G. W. *Sol-Gel Science, The Physic and Chemistry of Sol-Gel Processing*, Academic Press, New York, 1990.
(19) Haruta, M.; Kageyama, H.; Kamijo, N.; Kobayashi, T.; Delannay, F. *Stud. Surf. Sci. Catal.* **1988**, *44*, 33.
(20) Herrmann, J. M.; Mansot, J. L. *J. Catal.* **1990**, *121*, 340.
(21) Herrmann, J. M.; Disdier, J.; Pichat, P.; Fernandez, A.; Gonzalez-Elipe, A.; Munuera, G.; Leclercq, C. *J. Catal.* **1991**, *132*, 490 and references therein.
(22) Fernandez, A.; Gonzalez-Elipe, A. R.; Real, C.; Caballero, A.; Munuera, G. *Langmuir* **1993**, *9*, 121.

0897-4756/93/2805-0994$04.00/0

induced deposition occurs selectively on TiO_2 in a mechanical mixture of TiO_2/SiO_2 support.[20] Colloidal metal particles have also been prepared by the photoreduction of metal–organic compounds in the presence of silanes.[23] The photolysis of $(\eta^5\text{-}C_5H_5)PtMe_3$ in the presence of the silane $HMe_2SiOSiMe_3$ resulted in formation of an active hydrosilylation catalyst which was most likely to be a heterogeneous platinum colloid.[23] However, photolysis is not necessary in some systems where the silane can act as the reducing agent.[24–27]

We have been interested in the formation of highly dispersed rhodium particles derived from organometallic precursors either in colloidal solution or supported on metal oxide supports for their catalytic hydrogenation activity[9–11,28–31] and have prepared 2–4-nm-sized rhodium particles by photolysis of organometallic compounds.[11] As a continuation of these studies, we report here a model study in which nanometer-sized rhodium particles are dispersed on oxide supports at ambient temperature.

Experimental Section

General Procedures and Instrumentation. All manipulations were carried out under a dinitrogen atmosphere using standard Schlenk techniques.[32] Hydrocarbon and ethereal solvents were predried over sodium, distilled from sodium benzophenone ketyl, and stored over 4-Å molecular sieves. The compound $[(C_2H_4)_2RhOEt]_2{\cdot}H_2O$ was prepared by the method previously described.[11] Spherical SiO_2 particles were prepared according to the method of Stober et al.[33] and chosen to facilitate characterization of the surface metal particles by TEM. Rod-shaped particles of β-FeOOH were prepared by modification of the literature procedure.[34] Thermogravimetric analyses (TGA) were performed on a Perkin-Elmer TGA 7 instrument. Scanning electron microscopy (SEM) was obtained with a Hitachi S-800 instrument. Transmission electron microscopy (TEM) was performed on a JEOL 2000-FX isntrument operating at 200 keV. Electron diffraction data revealed the presence or absence of crystallinity in the samples as described for each individual case. However, the extent of crystallinity (i.e. the percent crystalline content) was not determined. Both SEM and TEM samples were prepared by redispersing the powder formed as reaction product in the appropriate solvent to form a black suspension from which a silicon wafer could be dip-coated for SEM or a 3-mm carbon-coated copper grid could be dip-coated for TEM for all samples. X-ray powder diffraction data were collected on the PVD-V Scintag X-ray diffractometer using a smear mount method to load a uniform and thin layer of sample onto a piece of glass of size 3 × 3 cm^2. Surface areas (BET) were measured by nitrogen adsorption. Thermal annealing for the product was carried out on a scale of approximately 20–40 mg by placing the powder in a quartz boat inside a quartz furnace tube with both ends capped under dinitrogen atmosphere. The tube was loaded into a tube furnace, evacuated to 10^{-2} Torr, and heated slowly to the specific temperature for the desired length of time.

Syntheses. *β-FeOOH Particles.* The compound $FeCl_3{\cdot}6H_2O$, 3.52 g (0.050 mol) in 0.1 N HCl was dissolved in distilled water, and the solution was filtered and diluted to 500 mL. The solution was transferred into a Erlenmeyer flask and sealed with a screw cap. The Erlenmeyer flask was placed in a preheated oven and kept at 100 °C for 24 h. After aging, the solution was separated by centrifuging, six times washed by distilled water and three times by acetone, and dried at ambient temperature. The yield of orange-tan product was 2.162 g, 49%. The average particle size is 250 nm in length and 55 nm in width. BET surface area is 21.7 m^2/g. The product was confirmed mainly to be β-FeOOH by X-ray powder diffraction, in which the patterns were consistent with literature.[35] However, there was contamination of very small amount of cubic $\alpha\text{-}Fe_2O_3$ as determined by TEM and electron diffraction.

Disperson of Rh on SiO_2. (a) *Synthesis of 2.4 wt % Rh on SiO_2*: A Schlenk flask was charged with 200 mg (3.33 mmol) of SiO_2 spheres, 10 mg (0.023 mmole) of $[(C_2H_4)_2RhOEt]_2{\cdot}H_2O$ and a stir bar under a N_2 atmosphere. Then, 20 mL of THF was added. The suspension was dispersed by an ultrasonic cleaner for a minute and stirred at room temperature in the dark for about 30 min and was irradiated by a mercury lamp for 3 h. Then the product was separated by filtration, washed with acetone, and dried in air. The BET surface area is 13.7 m^2/g.

(b) *Synthesis of 11.8 wt % Rh on SiO_2*: A Schlenk flask was charged with 253 mg (4.21 mmol) of SiO_2 spheres, 70 mg (0.164 mmol) of $[(C_2H_4)_2RhOEt]_2{\cdot}H_2O$ and a stir bar under a N_2 atmosphere. Then, 20 mL of THF was added. The suspension was dispersed by an ultrasonic cleaner for a minute and stirred at room temperature in the dark for about 1 h and was irradiated by a mercury lamp for 1.5 h. The solution changed color from yellow to black. Then the final black product was separated by filtration, washed with acetone, and dried in air. A small amount of black Rh was noticed at the inside of the Schlenk flask wall where the light beam was incident.

Dispersion of Rh on β-FeOOH. (a) *Synthesis of 2.4 wt % Rh on β-FeOOH*: A Schlenk flask was charged with 200 mg (2.25 mmole) of β-FeOOH, 10 mg (0.023 mmol) of $[(C_2H_4)_2RhOEt]_2{\cdot}H_2O$ and a stir bar under a N_2 atmosphere. Then, 15 mL of THF was added. The suspension was dispersed by an ultrasonic cleaner for a minute and stirred at room temperature in the dark for about 30 min and was irradiated by a mercury lamp for 2 h. The product was separated by filtration, washed with acetone, and dried in air. The BET surface area is 28.1 m^2/g.

(b) *Synthesis of 11.4 wt % Rh on β-FeOOH*: A Schlenk flask was charged with 150 mg (1.69 mmol) of β-FeOOH, 40 mg (0.0939 mmol) of $[(C_2H_4)_2RhOEt]_2{\cdot}H_2O$, and a stir bar under N_2 atmosphere. Then, 15 mL of THF was added. The suspension was dispersed by a ultrasonic cleaner for a minute and stirred at room temperature in the dark for about 30 min and was irradiated by a mercury lamp for 3 h. The product was separated by filtration, washed with acetone, and dried in air. The BET surface area is 27.0 m^2/g.

Studies of the Reaction Pathway. (a) *Photolysis*: Each of three 5 mm NMR tubes was charged with 6 mg, 0.014 mmol of $[(C_2H_4)_2RhOEt]_2{\cdot}H_2O$. In the first and second tubes, 30 mg, 0.338 mmol of β-FeOOH and 30 mg, 0.499 mmol, of SiO_2 were added, respectively. Then 0.35 mL of C_6D_6 was added to all three NMR tubes. The third NMR tube did not contain any metal oxide and served as the control. The mixtures were dispersed by immersing the NMR tubes in an ultrasonic cleaning bath for 1 min and then irradiated with a Hg lamp for various times. The changes in the reaction mixture were monitored as a function of time by ^1H NMR spectroscopy.

(b) *Surface reaction*: A Schlenk flask was charged with 200 mg, (2.25 mmol) of rod-shaped β-FeOOH, 40 mg, 0.0939 mmol of $[(C_2H_4)_2RhOEt]_2{\cdot}H_2O$, and a stir bar. Then, 20 mL of THF was added, and the suspension dispersed by immersion in an ultrasonic cleaning bath. The mixture was stirred in the dark for 1.5 h and filtered, and the residue washed with THF four times and then redispersed in 10 mL of THF. The suspension was again dispersed with an ultrasonic cleaner and irradiated with a Hg lamp for 3 h. The rod-shaped β-FeOOH particles were then separated by filtration, washed with acetone, and dried in air. No visual color change was observed on the surface of the

(23) Boardman, L. D.; *Organometallics* **1992**, *11*, 4194.
(24) Tour, J. M.; Pendalwar, S. L. *Tetrahedron Lett.* **1990**, *31*, 4719.
(25) Lewis, L. N.; Uriarte, R. J.; Lewis, N. *J. Mol. Catal.* **1991**, *66*, 105.
(26) Lewis, L. N.; Sy, K. G.; Donahue, P. E. *J. Organomet. Chem.* **1992**, *427*, 165.
(27) Lewis, L. N.; Lewis, N. *Chem. Mater.* **1989**, *1*, 106.
(28) Duan, Z.; Hampden-Smith, M. J.; Sylwester, A. P. *Chem. Mater.* **1992**, *4*, 1146.
(29) Anderson, S. L.; Datye, A. K.; Wark, T. A.; Hampden-Smith, M. J. *Catal. Lett.* **1991**, *8*, 345.
(30) Wark, T. A.; Gulliver, E. A.; Hampden-Smith, M. J.; Rheingold, A. L. *Inorg. Chem.* **1990**, *29*, 4360.
(31) Rousseau, F.; Duan, Z.; Hampden-Smith, M. J.; Datye, A. *Mater. Res. Soc. Symp. Proc.* **1992**, *271*, 633.
(32) Shriver, D. F.; Drezden, M. A. *The Manipulation of Air-Sensitive Compounds*, 2nd; Wiley-Interscience: New York, 1986; p 78.
(33) Stober, W.; Fink, A. *J. Colloid Interface Sci.* **1968**, *26*, 62.
(34) Matijevic, E.; Scheiner, P. *J. Colloid Interface Sci.* **1978**, *63*, 509.
(35) Murad, E. *Clay Miner.* **1979**, *14*, 273.

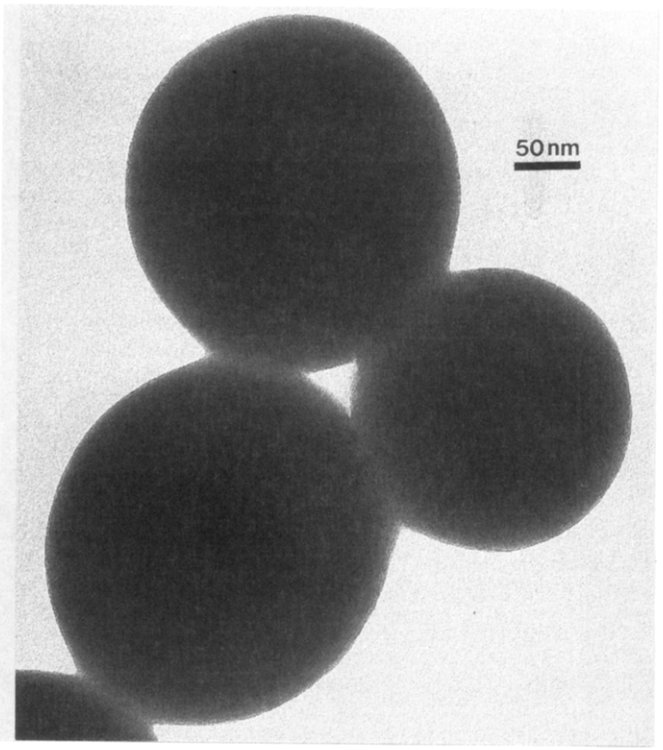

Figure 1. TEM of uncoated silica spheres.

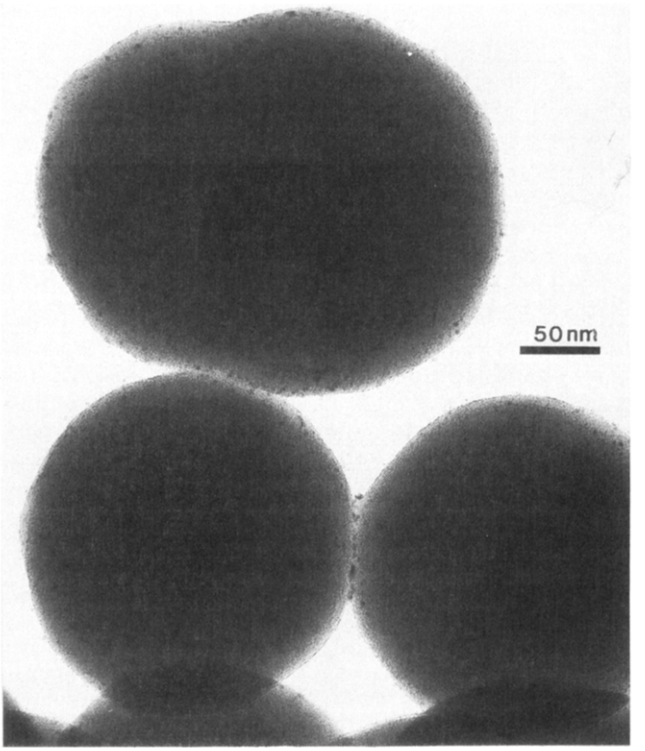

Figure 2. TEM of lower Rh content coated silica spheres.

particles, and energy-dispersive spectroscopy showed no evidence for the presence of Rh.

Results and Discussion

Amorphous, spherical SiO_2 particles and rod-shaped, crystalline β-FeOOH were chosen as support materials. Although the morphology of these materials does not give rise to extremely high surface areas which are necessary for catalytic applications, they were chosen because relatively small, well-defined particles of each can be prepared which aid characterization, particularly by electron microscopy. Furthermore, β-FeOOH is a prototypical example of a thermally sensitive metal oxide support. Rhodium was chosen as support material because we are interested in examining methods to prepare highly dispersed Rh particles *via* molecular routes for catalytic applications related to coal liquefaction.

The SiO_2 particles were prepared by the literature methods, and rod-shaped, crystalline β-FeOOH supports were prepared by the methods reported in the Experimental Section. These materials were characterized by microscopy and diffraction techniques prior to use. The β-FeOOH particles were found to be single crystals as determined by electron diffraction[36-39] and found to exhibit thermal dehydration behavior analogous to that reported in the literature.[40-44] We observed that the morphology of the rod-shaped β-FeOOH particles is retained on heating to 400 °C for 3 h *in vacuo*, but that the sample is thermally dehydrated to form crystalline α-Fe_2O_3. Highly dispersed Rh particles on SiO_2 and β-FeOOH as supports were prepared by irradiating a THF solution of $[(C_2H_4)_2Rh(OEt)]_2 \cdot H_2O$ compound[11] with a UV source. It has been demonstrated previously that this complex is photoreduced to Rh. For each support material, an experiment was carried out to disperse Rh particles on the surface with both a low and a high weight % Rh.

A 2.4 wt % Rh solution of $[(C_2H_4)_2Rh(OEt)]_2 \cdot H_2O$ was irradiated in the presence of a rapidly stirred THF suspension of amorphous ~250-nm SiO_2 spheres. After irradiation, the yellow solution became colorless and the white silica spheres became gray and could be separated from the solution by filtration. Transmission electron micrographs of the silica spheres before and after photolysis are shown in Figures 1 and 2, respectively. After photolysis, black particles with average particle size of 2–4 nm in diameter were uniformly dispersed over the surface of the silica spheres. Energy-dispersive spectroscopy (EDS) revealed the presence of silicon and rhodium. The average rhodium loading of 1.3 wt % (EDS) was similar to the value expected based on the solution Rh content.

In an experiment with a higher Rh content, TEM revealed that the Rh particle dispersion was inhomogeneous, as shown in Figure 3. Agglomerates of ~2-nm-sized rhodium particles were visible over the surface of the silica spheres, probably due to the high concentration of the rhodium precursor. EDS revealed that the average rhodium loading in the homogeneous area was 16.3 wt % and that the agglomerates were rhodium rich. Electron diffraction exhibited a single diffuse ring with a d spacing of 2.2 Å, consistent with that of fcc rhodium metal. X-ray powder diffraction of this sample showed the presence of a broad peak corresponding to a d spacing of 2.2 Å. After heating to 400 °C for 2 h *in vacuo*, the peaks sharpened and corresponded only to the peaks for fcc Rh. To establish the homogeneity of these sample, they were examined by scanning electron microscopy (SEM). These experiments

(36) Gallagher, K. J. *Nature* **1970**, *226*, 1225.
(37) Knowles, J. E., *IEEE Trans.* **1971**, *MAG-14(5)*, 858.
(38) Naylor, D. L. *J. Mater. Res.* **1992**, *7*, 2288.
(39) Sueyoshi, T.; Naono, H.; Amemiya, M. *IEEE Trans.* **1987**, *MAG-23(1)*, 80.
(40) Naono, H.; Fujiwara, R.; Sugioka, H.; Sumiya, K.; Yanazawa, H. *J. Colloid Interface Sci.* **1982**, *87*, 316.
(41) Howe, A. T.; Gallagher, K. J. *J. Chem. Soc., Faraday Trans.* **1975**, *171*, 22.
(42) Ishikawa, T.; Inouye, K. *Bull. Chem. Soc. Jpn.* **1972**, *45*, 2350.
(43) Ishikawa, T.; Inouye, K. *Bull. Chem. Soc. Jpn.* **1975**, *48*, 1580.
(44) Naono, H.; Nakai, K. *J. Colloid Interface Sci.* **1989**, *128*, 146.

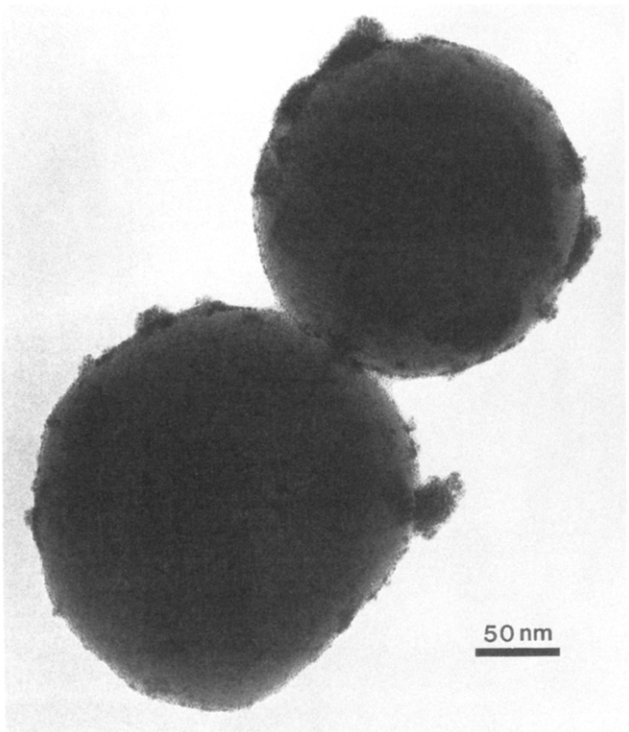

Figure 3. TEM of higher Rh-content coated silica spheres.

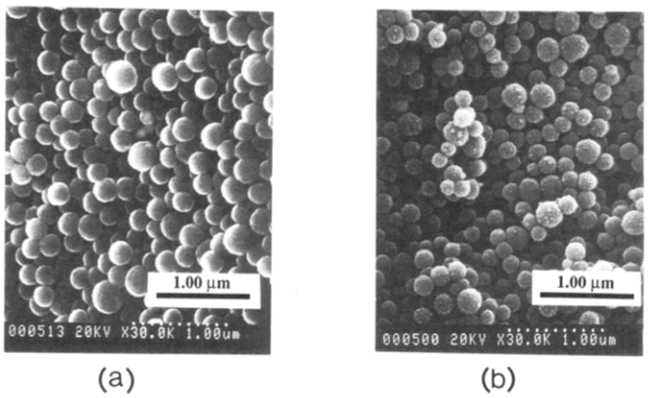

Figure 4. SEM data for Rh on SiO_2 for (a) low Rh and (b) high Rh loadings. The high Rh loading sample was heated to 400 °C *in vacuo* for 2 h.

revealed that the surface of the SiO_2 particles was roughened compared to uncoated particles and that the SiO_2 spheres were homogeneously coated. Typical micrographs are shown in Figure 4. The resolution of the scanning electron microscope was not sufficient to reveal the presence of the low weight loading of Rh on the SiO_2 spheres, although the presence of Rh could be detected by EDS.

Two different rhodium loadings on single-crystal β-FeOOH samples were prepared by similar methods as described for silica. In both cases, the color of the original bright yellow solution changed to colorless after photolysis and the yellow-orange powder changed to brown or brown-black for low & high Rh loadings, respectively. Figure 5 shows the electron micrograph of the β-FeOOH particles before photolysis and Figure 6 and 7 show the β-FeOOH particles after photolysis for the low and high Rh loadings, respectively. For the low weight loading sample, the approximately 2–4-nm-sized Rh particles primarily aggregated at the ends of the rod-shaped particles, see Figure 6. The weight loading of 2.4 wt % and the presence of Rh

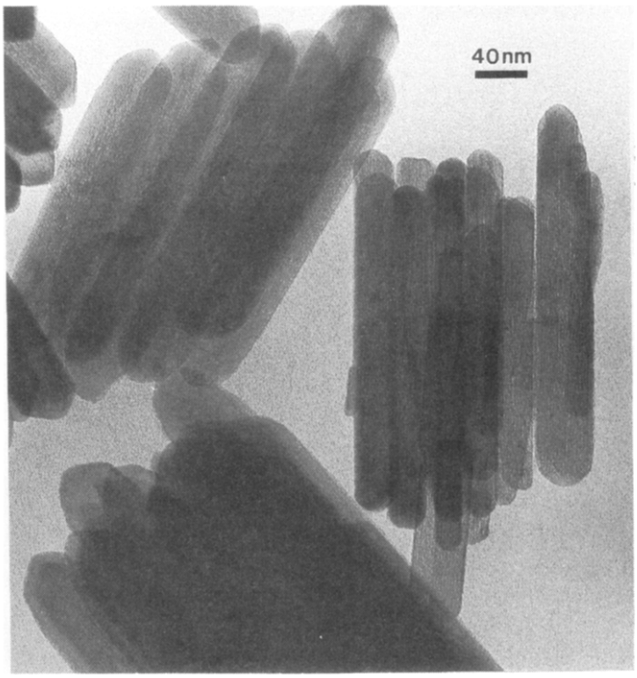

Figure 5. TEM of uncoated rod-shaped β-FeOOH.

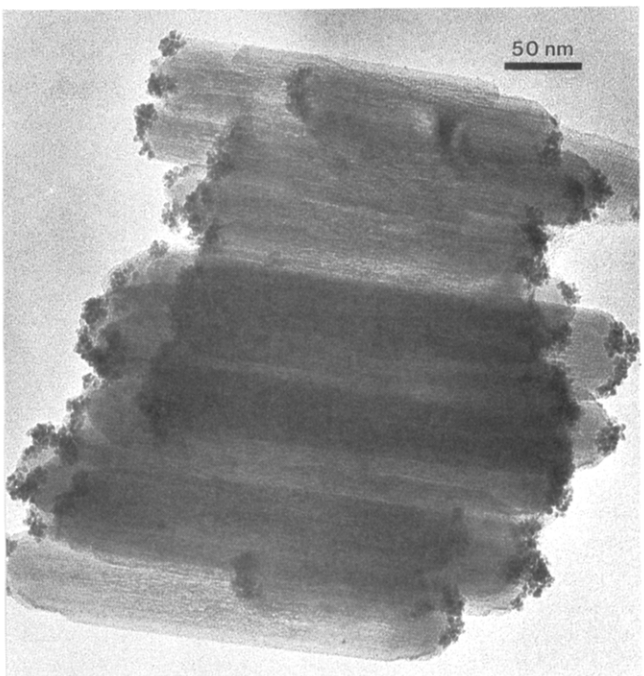

Figure 6. TEM for low weight-loading Rh-coated β-FeOOH particles.

were confirmed by EDS. For the higher Rh weight loading, it can be seenthat black aggregates consisting of 2–4-nm-sized particles were dispersed over the surface and the ends of rodlike β-FeOOH particles, Figure 7. EDS showed the presence of rhodium and iron and the average rhodium loading of 17.0 wt %, higher than the expected value of 11.4 wt % based on solution Rh content probably because the Rh particles aggregate. The individual β-FeOOH particles were still crystalline, as shown by electron diffraction for the upper right particles in Figure 7. Electron diffraction (in a different location) also exhibited a single diffuse ring at a *d* spacing of 2.2 Å, corresponding to fcc rhodium metal. However, X-ray powder diffraction of this sample exhibited only peaks due to β-FeOOH. Low-resolution SEM data for the two different Rh weight

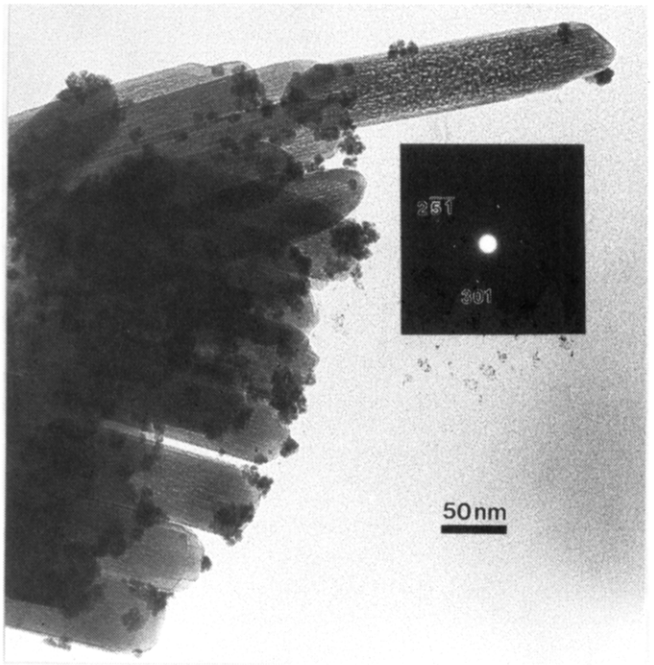

Figure 7. TEM and electron diffraction of high weight-loading Rh-coated β-FeOOH particles.

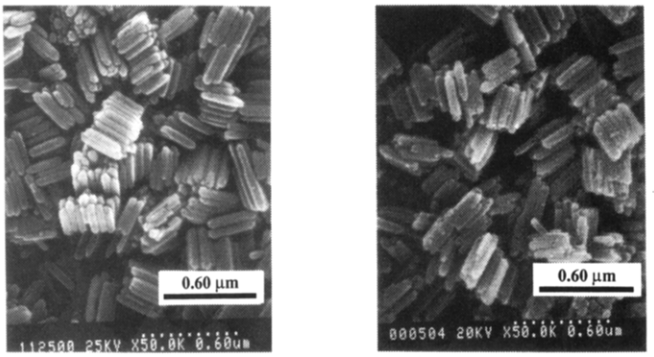

Figure 8. (a) SEM data for Rh on β-FeOOH with (a) low Rh and (b) high Rh loadings.

loadings on β-FeOOH are shown in Figure 8. These micrographs reveal macroscopic features of the samples and show that the morphology of the β-FeOOH has been retained and that in the case of the high weight loading that the Rh is confined to the surface of the particles. The BET surface areas of the Rh-coated β-FeOOH particles were both higher than the uncoated materials.

In an attempt to resolve the issue of whether the precursor is photochemically reduced in homogeneous solution or after reaction with the support surface hydroxyl groups, a number of control experiments were carried out. Independent studies of the photolysis of $[(C_2H_4)_2Rh(OEt)]_2 \cdot H_2O$ in benzene-d_6 revealed the formation of ethylene, ethanol, ethane and acetaldehyde by multinuclear NMR spectroscopy and 2–4-nm-sized rhodium particles by TEM. The changes in the ^1H NMR spectrum of a solution of $[(C_2H_4)_2Rh(OEt)]_2 \cdot H_2O$ in benzene-d_6 as a function of the irradiation time are shown in Figure 9. The species formed can be explained by mechanisms involving fundamental steps commonly associated with

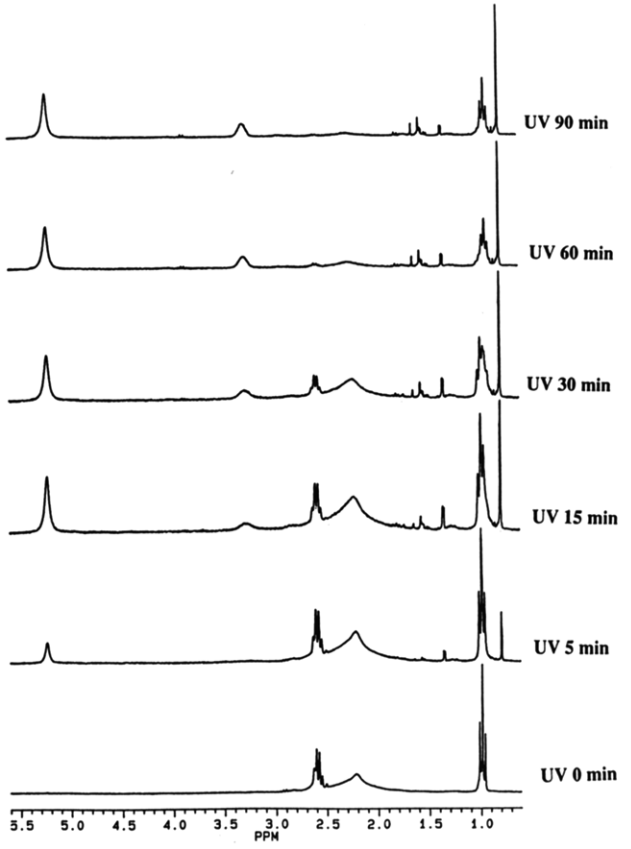

Figure 9. ^1H NMR spectra showing the photochemical decomposition of $[(C_2H_4)_2Rh(OEt)]_2 \cdot H_2O$ in benzene-d_6 as a function of the irradiation time.

Scheme I. Proposed Reaction Pathways That Can Account for the Formation of the Byproducts Observed on Photolysis of $[(C_2H_4)_2Rh(OEt)]_2 \cdot H_2O$ in Benzene-d_6

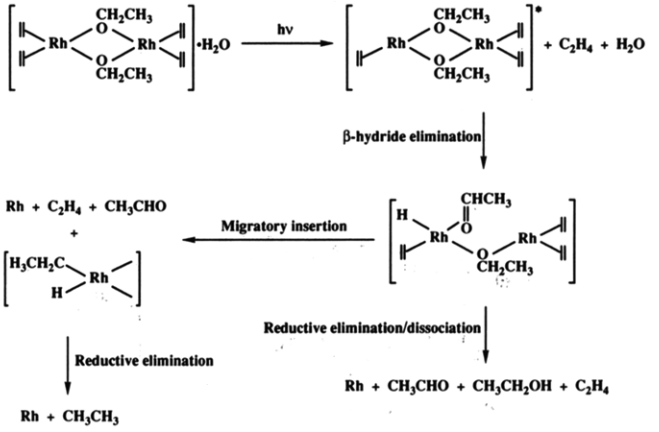

organometallic reactions, namely, β-hydride elimination, reductive elimination and migratory insertion as proposed in Scheme I.[45] It seems likely that the chromophore is associated with the Rh–ethylene bond since the corresponding 1,5-cyclooctadiene complex, $[(1,5\text{-COD})Rh(OEt)]_2$ is stable under similar photolysis conditions. Furthermore, the complex $[(C_2H_4)_2Rh(Cl)]_2$ is significantly less photolabile than $[(C_2H_4)_2Rh(OEt)]_2 \cdot H_2O$, perhaps as a result of the absence of β-hydrogens in the case of the chloride complex. The photodissociation of the coordinated olefin ligand would produce a vacant coordination site necessary for subsequent reactions. This is consistent with the experimental observation that ethylene is rapidly

(45) Collman, J. P.; Hegedus, L. S.; Norton, J. R.; Finke, R. G. *Principles and Applications of Organotransition Metal Chemistry*; University Science Books: Mill Valley, CA, California, 1987.

liberated on photolysis; see Figure 9. A comparison of the rate of photochemical decomposition of $[(C_2H_4)_2Rh(OEt)]_2 \cdot H_2O$ in the presence or absence of SiO_2 was made by ^1H NMR spectroscopy in C_6D_6 solution. This study revealed that the rate constants for the rate of loss of the Rh starting material were similar, in the presence of SiO_2, 0.028/min ($t_{1/2}$ = 25 min), in the absence of SiO_2, 0.024/min, $t_{1/2}$ = 29 min. When $[(C_2H_4)_2Rh(OEt)]_2 \cdot H_2O$ was irradiated in benzene-d_6 solution in the presence of β-FeOOH, the paramagnetism present resulted in extensive broadening of all the peaks in the ^1H NMR spectrum and precluded comparison of the rates of photochemically-induced decomposition in the presence and absence of this support. However, analysis of the soluble byproducts by ^1H NMR spectroscopy revealed that no starting material remained and that byproducts identical to those observed in control experiments were present.

To probe the nature of interaction of $[(C_2H_4)_2Rh(OEt)]_2 \cdot H_2O$ with the surface hydroxyl groups further, a solution of the precursor and β-FeOOH particles was stirred in THF in the dark and then filtered. The β-FeOOH particles were then re-suspended in THF and irradiated for 3 h. No color change was observed on the surface of the particles, and no evidence for the presence of Rh was observed by EDS. In other experiments, we have demonstrated[29] that it is possible to observe the low concentration of Rh present after reaction of a metal–organic Rh molecule containing *terminal* alkoxide ligands $(((1,5\text{-}COD)Rh)_2Sn(OEt)_6)$ with surface hydroxyl groups. In this case, the *bridging* alkoxide groups may be less labile.

As a result of these observations, it seems most likely that $[(C_2H_4)_2Rh(OEt)]_2 \cdot H_2O$ photochemically decomposes in homogeneous solution to form 2–4-nm sized Rh crystallites which subsequently adsorb on the metal oxide support surface. This mechanism is quite different from previous reports of the photochemically induced deposition of metals on metal oxide surfaces described in the introduction, where the chromophore is the metal oxide surface, such as TiO_2, rather than the metal-containing precursor. Both methods of formation of metal particles have their advantages and disadvantages. The advantage of surface-induced photochemical decomposition is that selective deposition on one surface in the presence of another is possible. The advantages of photochemical decomposition of the metal–organic precursor in homogeneous solution to produce metal particles on supports are low temperature and the ability to disperse the metal particles over the entire surface. This technique is attractive for preparation of highly dispersed particles for catalyst applications and other nanostructured materials.[46] Further studies are in progress to determine the hydrogenation activity of the materials described herein.

Acknowledgment. This work was funded by DOE Contract DE-AC04-76DP00789. M.H.-S. thanks Johnson-Matthey for the loan of $RhCl_3 \cdot xH_2O$ through the Johnson-Matthey Precious Metals Loan Program, the NSF Chemical Instrumentation program for the purchase of a high-field NMR spectrometer, Dr. Lu-Min Wang for assistance in obtaining the TEM data, Leo Archer and Dongshui Zeng for X-ray powder diffraction data, and Bill Ackerman for surface area measurements. We thank ONR for analytical facilities and Dr. A. Sylwester for helpful discussions.

(46) Dagani, R. *Chem. Eng. News* **1992**, Nov 23, 18.